Journal of Thermal Analysis and Calorimetry, Vol. 94 (2008) 1, 63–67

NICKEL FERRITE NANOPARTICLES SYNTHESIS FROM NOVEL FUMARATO–HYDRAZINATE PRECURSOR

A. More[1], *V. M. S. Verenkar*[1] *and S. C. Mojumdar*[2,3]*

[1]Department of Chemistry, Goa University, Goa 403206, India
[2]Department of Chemical Engineering and Applied Chemistry, University of Toronto, 200 College St., Toronto, ON, M5S 3E5, Canada
[3]University of New Brunswick, Saint John, NB, E2L 4L5, Canada

Nickel ferrite is technologically important magnetic material extensively used in high frequency applications such as microwave device due to its high resistivity and sufficiently low losses. It also finds application in the ferrofluids technology. Therefore, ultrafine nickel ferrite was prepared by autocatalytic combustion of novel nickel ferrous fumarato–hydrazinate precursor. The precursor was characterized by IR, AAS, TG and DTA, and a chemical formula of $NiFe_2(C_4H_2O_4)_3{\cdot}6N_2H_4$ was fixed. This precursor once ignited with a burning splinter at room temperature, glows and the glow spreads over the entire bulk completing the autocatalytic combustion of the precursor to ultrafine ferrite. The single phase formation of ultrafine nickel ferrite was confirmed by XRD, IR spectra and TEM. The average particle size of the ultrafine ferrite was found to be ~20 nm by TEM. The observed lower value of saturation magnetization for nickel ferrite was due to the superparamagnetic nature of the particles, which increased with the increasing sintering temperature. The ultrafine nickel ferrite was then sintered at 1000°C for 5 h and was characterized by XRD, IR spectra, SEM and TEM. The variation of resistivity, Seebeck coefficient and a.c. susceptibility as a function of temperature was measured for $NiFe_2O_4$ and the results are discussed.

Keywords: *AAS, DTA, IR, nickel ferrite magnetic semiconductor nanoparticles, SEM, TEM, TG, XRD*

Introduction

Synthesis of solids, possessing desired structures, stoichiometry and properties continues to be a challenge to chemists, material scientists and engineers [1]. Formation of solids by ceramic method is controlled by the diffusion of atoms and ionic species through reactants and products and thus requires repeated grinding, pelletising and calcination of reactants for longer duration at high temperatures. Attempts have been made recently to bypass diffusion control problems of solid synthesis using various innovative synthetic strategies. One such approach is, 'combustion synthesis'. Recently many such combustion synthesis of metal and mixed metal oxides using metal hydrazine complexes of oxalate [2], sulphite [3], formate [4], acetate [5], propionate [6], hydrazidocarboxylate [7], malonate and succinate [8–10], maleate and fumarate [9, 11], tartrate [11] and malate [12] have been studied. There has been considerable interest among researchers in the study of organic-inorganic materials including hydrazine derivatives of metal carboxylates since they serve as precursors to fine particle oxide materials relatively at much lower temperatures and also in their characterization using various techniques such as TG, DTA, SEM, TEM, XRD, AAS and FTIR spectroscopy [13–50].

In the present investigation the combustion synthesis of nickel ferrite nanoparticles, using novel fumarato-hydrazinate precursor has been studied as nickel ferrite is a technologically important material extensively used in high frequency applications such as microwave devices due to their high resistivity and sufficiently low losses. It also finds application in the ferrofluid technology.

Experimental

Preparation

A requisite quantity of sodium fumarate in aqueous medium was stirred with hydrazine hydrate (99–100%) in an inert atmosphere for 2 h. To this solution, a stoichiometric amount of freshly prepared ferrous chloride solution mixed with nickel chloride was added dropwise with constant stirring in an inert atmosphere. The yellow colored precipitate thus obtained was filtered, washed with ethanol, dried with diethyl ether and then stored in vacuum desiccators.

* Author for correspondence: scmojumdar@yahoo.com

1388–6150/$20.00
© 2008 Akadémiai Kiadó, Budapest
Akadémiai Kiadó, Budapest, Hungary
Springer, Dordrecht, The Netherlands

These precursors once ignited decompose autocatalytically to form ferrite at lower temperature. For this autocatalytic decomposition, the precursor was first spread over a petridish and a burning splinter was brought near to it, when small portion of it caught fire. A red glow that formed spread over the entire bulk completing the total decomposition of the precursor in an ordinary atmosphere. This 'as prepared' ultrafine nickel ferrite powder was then pelletised putting a pressure of 7 T inch^{-2} for 3 min and sintered at 1000°C for 5 h.

Characterization

The hydrazine content in the precursor was determined by volumetric analysis using standard 0.025 M KIO_3 solution under Andrew's conditions [51]. The metal contents were determined using an atomic absorption spectrophotometer model 201 Chemita. The structure and phase purity of the nickel ferrite ('as prepared' as well as sintered) was determined by a Philips X-ray diffractometer model PW 1710 with CuK_α radiations and Ni filter. The morphology of 'as prepared' and sintered nickel ferrite was observed by transmission electron microscopy using a JEM 2000 CX electron microscope and scanning electron microscopy using a JEOL-JSM 5600LV electron microscope, respectively. Simultaneous thermogravimetric and differential thermal analysis of precursor was recorded on a STA 1500 thermal analyzer up to 600°C, at a heating rate of 10°C min^{-1}. The isothermal and total mass loss studies of the precursor were carried out along with hydrazine estimation at various predetermined temperatures. Infrared spectral analysis of the precursor and the ferrite was done using a Shimadzu FTIR, model 8101 A. The saturation magnetization of the ferrite sintered at different temperatures was measured on alternating current hysteresis loop tracer described by Likhite *et al.* [52] and supplied by M/s Arun Electronics, Mumbai, India. The variation of a.c. susceptibility, resistivity and Seebeck coefficient as a function of temperature was measured for $NiFe_2O_4$, the same way as described elsewhere [53].

Results and discussion

A chemical formula of $NiFe_2(C_4H_2O_4)_3{\cdot}6N_2H_4$ for nickel ferrous fumarato-hydrazinate precursor has been fixed based on the total percentage mass loss and percentages of hydrazine, nickel and iron which match closely with the calculated ones. The precursor is found to loose hydrazine ~150°C when heated isothermally. The infrared spectra of the precursor show three bands in the region 3250–3450 cm^{-1} due to the N–H stretching frequencies and in the range of 1560–1590 cm^{-1} due to NH_2 deformation. The N–N stretching frequency is observed at 980 cm^{-1} which confirms the bidentate bridging nature of hydrazine ligand [8, 54]. The asymmetric and symmetric stretching frequencies of the carboxylate ion in the precursor are seen at 1635 and 1375 cm^{-1}, respectively with $\Delta\nu$ (ν_{asy}–ν_{sym}) separation of 260 cm^{-1} indicating the monodentate linkage of both carboxylate groups in the dianions [6, 8, 11]. Thus, the fumarate dianions in the complex coordinate to the metal as bidentate ligand via both carboxylate groups. These results suggest the formation of nickel ferrous fumarato–hydrazinate complex.

The complex decomposes autocatalytically at room temperature, once ignited, to give ultrafine

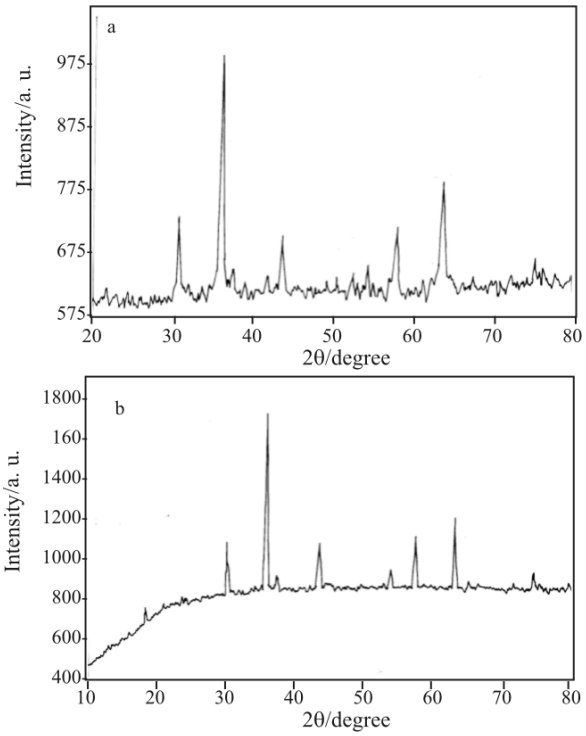

Fig. 1 XRD of $NiFe_2O_4$ a – freshly prepared and b – sintered

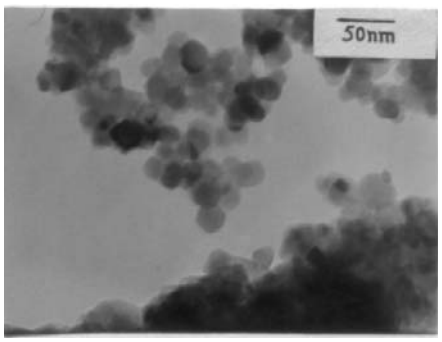

Fig. 2 TEM of freshly prepared $NiFe_2O_4$

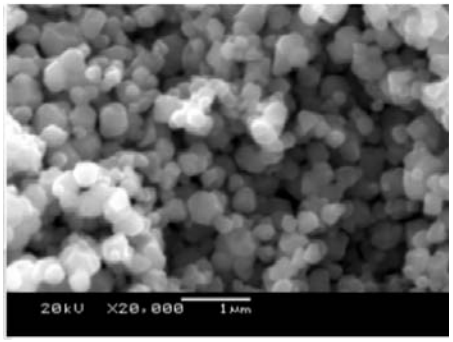

Fig. 3 SEM of sintered $NiFe_2O_4$ obtained from $NiFe_2(C_4H_2O_4)_3{\cdot}6N_2H_4$

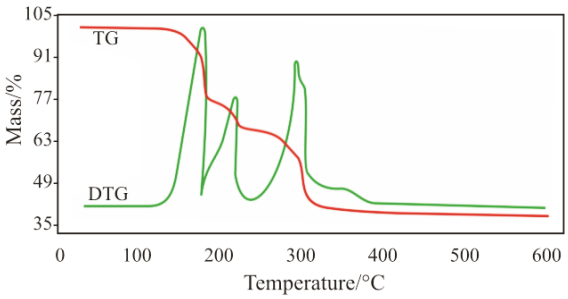

Fig. 4 TG-DTA curves of nickel ferrous fumarato-hydrazinate ($NiFe_2(C_4H_2O_4)_3{\cdot}6N_2H_4$) precursor

nickel ferrite (as prepared). The X-ray diffraction of 'as prepared' nickel ferrite (Fig. 1) not only confirms the single phase formation of the ferrite but also the ultrafine nature.

The morphology of 'nanosized as prepared' and sintered nickel ferrite was observed by transmission electron microscopy (Fig. 2) and scanning electron microscopy (Fig. 3). The TEM (Fig. 2) of 'nanosized as prepared' nickel ferrite shows the average particle size of ~20 nm. The scanning electron micrograph of sintered nickel ferrite show uniformly crystallized particles with majority of them is in the size of 500 nm (Fig. 3).

TG-DTA curves of nickel ferrous fumarato-hydrazinate ($NiFe_2(C_4H_2O_4)_3{\cdot}6N_2H_4$) precursor are given in Fig. 4. The TG curve indicates that it is thermally stable up to 140°C. Afterwards, the TG curve shows three mass loss steps. The first step between 140 and 170°C is attributed to the elimination of six hydrazine molecules. The second step took place between 170 and 225°C and is attributed, however, to the decomposition of one fumarate. The third step took place between 225 and 325°C. It is attributed, however, to the elimination of remaining two fumarates and formation of the $NiFe_2O_4$ nanoparticles.

The DTA curve for $NiFe_2(C_4H_2O_4)_3{\cdot}6N_2H_4$ precursor (Fig. 4) shows three exothermic peaks at 160, 210 and 290°C ascribed to the loss of $6N_2H_4$, one and two fumarates, respectively with the simultaneous formation of $NiFe_2O_4$ nanoparticles.

The saturation magnetization (in emu g^{-1}) of 'as prepared' nickel ferrite was found to be 28 emu g^{-1} which is lower than the reported value of 50 emu g^{-1} [55] for bulk $NiFe_2O_4$. The reason for the lower value of saturation magnetization is the high porosity and the small particle size of 'as prepared' nickel ferrite. It has been reported in the literature [56] that particles with higher surface area and very small size have lower magnetization values. The magnetization value of 'as prepared' nickel ferrite was found to increase with increasing sintering temperature and the sample sintered at 1000°C for 5 h was having the same value as reported for $NiFe_2O_4$. The X-ray diffraction data such as *d*-values and lattice parameter obtained from the XRD trace (Fig. 1) of sintered nickel ferrite match closely with the reported values [57, 58]. The IR spectra of the sintered $NiFe_2O_4$ show high frequency ν_1 and low frequency ν_2 bands at 600 and 430 cm^{-1} which match closely with the data reported for nickel ferrite by Waldron [59], thereby confirming the ferrite formation. The variation of electrical resistivity of sintered $NiFe_2O_4$ *vs.* temperature, show a decrease in resistivity with increasing temperature, as expected. The plot of logρ *vs.* $1/T$ indicates a change in slope at 585°C due to the switching of magnetic region from ferri to para. The plot of a.c. susceptibility against temperature of sintered nickel ferrite indicates that the sample contains predominantly multi-domain grains with a T_c of 588°C which matches closely with the reported one [60]. The variation of Seebeck coefficient as a function of temperature for sintered $NiFe_2O_4$ shows a negative sign of thermoemf suggesting the material is *n*-type semiconductor.

Conclusions

Nickel ferrite ultrafine particles have been prepared by the autocatalytic decomposition of the nickel ferrous fumarato–hydrazinate at room temperature, once ignited. The formation of 'as prepared' ultrafine nickel ferrite as well as sintered nickel ferrite was confirmed by X-ray diffraction as well as infrared analysis. The average particle size of 'as prepared' nickel ferrite was found to be 20 nm which increases maximum to 500 nm when sintered at 1000°C for 5 h. The Curie temperature of sintered $NiFe_2O_4$ measured by resistivity and a.c. susceptibility techniques are found to be close to each other as well as to the reported in the literature. Seebeck coefficient measurement of sintered $NiFe_2O_4$ displays *n*-type semiconducting behaviour. Thus, this work confirms that ultrafine nickel ferrite which finds applications in magnetic coating and ferrofluid technology can be produced by combustion synthesis using fumarato–

hydrazinate precursor at comparatively lower temperature. This resulted in atomic level reactivity at relatively lower sintering temperature and time, to give enhanced properties of the nanosize nickel ferrite.

Acknowledgements

The authors wishes to thank Prof. Arun Umarji and Dr. Nagesh Kini, MRC, IISc., Bangalore for TG-DTA measurements. Thanks are also due to Dr. G. N. Subbanna, MRC, IISc. and Mr. K. R. Kannan for taking TEM and SEM micrographs, respectively of the samples.

References

1 K. C. Patil, S. T. Aruna and S. Ekambaram, Curr. Opin. Sol. Stat. Mater. Sci., 2 (1997) 158.
2 D. Gajapathy, K. C. Patil and V. R. Pai Vernekar, Mater. Res. Bull., 17 (1982) 29.
3 J. S. Budkuley and K. C. Patil, Synth. React. Inorg. Met.-Org. Chem., 21 (1991) 709.
4 P. Ravindranathan and K. C. Patil, Thermochim. Acta, 71 (1983) 53.
5 G. V. Mahesh and K. C. Patil, Thermochim. Acta, 99 (1986) 188.
6 B. N. Sivasankar and S. Govindarajan, Z. Naturforsch., 1994, 49b, 950.
7 B. N. Sivasankar and S. Govindarajan, Ind. J. Chem., 33A (1994) 329.
8 B. N. Sivasankar and S. Govindarajan, Synth. React. Inorg. Met.-Org. Chem., 24 (1994) 1573.
9 V. M. S. Verenkar and K. S. Rane, 'Proc. 10th Nat. Symp. on Thermal Analysis', Mumbai, India 1995, p. 171.
10 V. M. S. Verenkar and K. S. Rane, 'Proc. 10th Nat. Symp. on Thermal Analysis', Mumbai, India 1995, p. 175.
11 S. Govindarajan, S. U. Nasrin Banu, N. Saravanan and B. N. Sivasankar, Proc. Indian Acad. Sci. (Chem. Sci.), 107 (1995) 559.
12 V. M. S. Verenkar and K. S. Rane, 'Proc. 12th Nat. Symp. on Thermal Analysis', Gorakhpur, India 2000, p. 194.
13 S. Y. Sawant, V. M. S. Verenkar and S. C. Mojumdar, J. Therm. Anal. Cal., 90 (2007) 669.
14 S. C. Mojumdar, M. Sain, R. Prasad, L. Sun and J. E. S. Venart, J. Therm. Anal. Cal., 90 (2007) 653.
15 M. Dováľ, M. Palou and S. C. Mojumdar, J. Therm. Anal. Cal., 86 (2006) 595.
16 H. S. Rathore, G. Varshney, S. C. Mojumdar and M. T. Saleh, J. Therm. Anal. Cal., 90 (2007) 681.
17 D. Czakis-Sulikowska, A. Czylkowska and A. Malinowska, J. Therm. Anal. Cal., 67 (2002) 667.
18 I. Janotka and L'. Krajči, CERAMICS-Silikaty, 39 (1995) 105.
19 K. G. Varshney, A. Agrawal and S. C. Mojumdar, J. Therm. Anal. Cal., 90 (2007) 721.
20 L'. Krajči, I. Janotka, I. Kraus and P. Jamnicky, Ceram. Silik., 51 (2007) 217.
21 G. Madhurambal, P. Ramasamy, P. A. Srinivasan and S. C. Mojumdar, J. Therm. Anal. Cal., 90 (2007) 673.
22 S. C. Mojumdar and L. Raki, J. Therm. Anal. Cal., 85 (2006) 99.
23 K. G. Varshney, A. Agrawal and S. C. Mojumdar, J. Therm. Anal. Cal., 90 (2007) 731.
24 S. C. Mojumdar, M. Melník and E. Jóna, J. Anal. Appl. Pyrolysis, 53 (2000) 149.
25 G. Madhurambal, S. Parthiban, G. Madhurambal, R. Dhanasekaran and S. C. Mojumdar, J. Therm. Anal. Cal., DOI: 10.1007/s10973-008-9181-1.
26 B. Borah and J. L. Wood, Can. J. Chem., 50 (1976) 2470.
27 S. C. Mojumdar, K. G. Varshney and A. Agrawal, Res. J. Chem. Environ., 10 (2006) 89.
28 H. S. Rathore, K. Ishratullah, C. Varshney, G. Varshney and S. C. Mojumdar, J. Therm. Anal. Cal., DOI: 10.1007/s10973-008-9191-z.
29 A. Ramadevi and K. Srinivasan, Res. J. Chem. Environ., 9 (2005) 54.
30 S. Meenakshisundaram, S. Parthiban, G. Madhurambal and S. C. Mojumdar, J. Therm. Anal. Cal., DOI: 10.1007/s10973-008-9182-0.
31 I. Janotka and L'. Krajči, Int. J. Cem. Comp. Light. Concr., 11 (1989) 221.
32 J. S. Skoršepa, K. Györyová and M. Melník, J. Thermal Anal., 44 (1995) 169.
33 D. Ondrušová, E. Jóna and P. Šimon, J. Therm. Anal. Cal., 67 (2002) 147.
34 E. Jóna, E. Rudinska, M. Sapietova, M. Pajtasova and D. Ondrusova, Res. J. Chem. Environ., 10 (2006) 31.
35 M. Kubranová, E. Jóna, E. Rudinská, K. Nemčeková, D. Ondrušová and M. Pajtášová, J. Therm. Anal. Cal., 74 (2003) 251.
36 E. Jóna, M. Hvastijová and J. Kohout, J. Thermal Anal., 41 (1994) 161.
37 D. Czakis-Sulikowska and A. Czylkowska, J. Thermal. Anal. Cal., 71 (2003) 395.
38 S. C. Mojumdar, M. Melník and E. Jóna, J. Therm. Anal. Cal., 56 (1999) 533.
39 R. A. Porob, S. Z. Khan, S. C. Mojumdar and V. M. S. Verenkar, J. Therm. Anal. Cal., 86 (2006) 605.
40 S. C. Mojumdar, L. Martiška, D. Valigura and M. Melník, J. Therm. Anal. Cal., 74 (2003) 905.
41 E. A. Ukraintseva, V. A. Logvinenko, D. V. Soldatov and T. A. Chingina, J. Therm. Anal. Cal., 75 (2004) 337.
42 S. C. Mojumdar, M. Melník and E. Jóna, J. Therm. Anal. Cal., 56 (1999) 541.
43 M. T. Saleh, S. C. Mojumdar and M. Lamoureux, Res. J. Chem. Environ., 10 (2006) 14.
44 S. C. Mojumdar, G. Madhurambal and M. T. Saleh, J. Therm. Anal. Cal., 81 (2005) 205.
45 K. G. Varshney, A. Agrawal and S. C. Mojumdar, J. Therm. Anal. Cal., 81 (2005) 183.
46 E. Jóna, E. Rudinská, M. Sapietová, M. Pajtášová, D. Ondrušová, V. Jorík and S. C. Mojumdar, Res. J. Chem. Environ., 9 (2005) 41.
47 S. C. Mojumdar, J. Miklovic, A. Krutošíková, D. Valigura and J. M. Stewart, J. Therm. Anal. Cal., 81 (2005) 211.
48 S. C. Mojumdar, Res. J. Chem. Environ., 9 (2005) 23–27.
49 G. Madhurambal, S. C. Mojumdar, S. Hariharan and P. Ramasamy, J. Therm. Anal. Cal., 78 (2004) 125.
50 S. C. Mojumdar, J. Therm. Anal. Cal., 64 (2001) 629.
51 A. I. Vogel, 'A Text Book of Qualitative Inorganic Analysis', ELBS and Longman, London 1978, p. 389.
52 S. D. Likhite, C. Radhakrishnamurthy and P. W. Sahasrabudhe, Rev. Sci. Instrum., 25 (1965) 302.

53 K. S. Rane, V. M. S. Verenkar and P. Y. Sawant, J. Mater. Sci., Mater. In Electronics, 10 (1999) 133.
54 A. Braibanti, F. Dallavalle, M. A. Pellinghelli and E. Leporati, Inorg. Chem., 7 (1968) 1430.
55 Y. Shi, J. Ding, X. Liu and J. Wang, J. Magn. Magn. Mater., 205 (1999) 249.
56 J. M. D. Coey and D. Khalafalla, Phys. Stat. Sol., 11 (1972) 229.
57 K. Suresh and K. C. Patil, J. Solid-State Chem., 99 (1992) 12.
58 D. Gajapathy and K. C. Patil, Mater. Chem. Phys., 9 (1983) 423.
59 R. D. Waldron, Phys. Rev., 99 (1955) 1727.
60 E. P. Wohlfarth, Ferromagnetic Materials, Vol.2, North-Holland Publishing Co., Amsterdam 1980, p. 201.

DOI: 10.1007/s10973-008-9189-6